IL-6 promotes low concentration of RANKL-induced osteoclastic differentiation by mouse BMMs through trans-signaling pathway

Wei Feng[1] · Panpan Yang[2,3] · Hongrui Liu[2,3] · Fan Zhang[2,4,6] · Minqi Li[2,3,5]

Abstract

The exact role of IL-6 in inflammatory osteoclast formation is still under debate. Our previous study demonstrated that IL-6 in the combination of sIL-6R significantly promoted low level of RANKL-induced osteoclast differentiation which was not affected by IL-6 alone. However, the precise molecular mechanisms underlying the regulation of sIL-6R-induced trans-signaling on osteoclast differentiation remains to be elucidated. Mouse bone marrow-derived monocytes (BMMs) were isolated and cultured with RANKL and IL-6/sIL-6R in the presence or absence of sgp130. TRAP staining and pit formation assay were used to visualize multinucleated giant osteoclasts and evaluate their bone resorption ability. Western blot and real time-PCR were applied to determine the activations of IL-6 signaling pathway and osteoclastogenesis- associated signaling pathways. The results showed that sIL-6R activation of IL-6 trans-signaling enhanced IL-6 signaling cascades and promoted low concentration of RANKL-induced osteoclasts formation and bone resorption by mouse BMMs. Furthermore, blocking IL-6 trans-signaling with sgp130 abrogated this promotive effect by suppressing NF-κB and JNK signaling pathways. In conclusion, sIL-6R-mediated trans-signaling pathway plays a decisive role in promotion of low level of RANKL-induced osteoclastic differentiation by IL-6/sIL-6R and targeting the IL-6 trans-signaling pathway may represent a potential strategy for inflammatory diseases with pathological bone resorption.

Keywords IL-6 · sIL-6R · sgp130 · Trans-signaling · Osteoclast

Introduction

IL-6 is a multifunctional cytokine which has been shown to be tightly implicated in various local and systematic inflammatory diseases with pathological bone loss, such as rheumatoid arthritis (RA), postmenopausal osteoporosis,

✉ Minqi Li
liminqi@sdu.edu.cn

Wei Feng
dentistfeng@live.com

Panpan Yang
c8yangpanpan720@163.com

Hongrui Liu
yf1blhr@126.com

Fan Zhang
zhfan@sdu.edu.cn

1 Department of Endodontics, Central Laboratory of Jinan Stomatological Hospital, Jinan Key Laboratory of Oral Tissue Regeneration, 250001 Jinan, Shandong, China

2 Center of Osteoporosis and Bone Mineral Research, Shandong University, 250012 Jinan, Shandong, China

3 Department of Bone Metabolism, School and Hospital of Stomatology, Cheeloo College of Medicine, Shandong Key Laboratory of Oral Tissue Regeneration & Shandong Engineering Laboratory for Dental Materials and Oral Tissue Regeneration, Shandong University, 250012 Jinan, Shandong, China

4 Department of Orthodontics, School and Hospital of Stomatology, Cheeloo College of Medicine, Shandong Key Laboratory of Oral Tissue Regeneration & Shandong Engineering Laboratory for Dental Materials and Oral Tissue Regeneration, Shandong University, 250012 Jinan, Shandong, China

5 Center of Osteoporosis and Bone Mineral Research, Department of Bone Metabolism, School of Stomatology, Shandong University, Shandong University, Wenhua West Road 44-1, 250012 Jinan, China

6 Center of Osteoporosis and Bone Mineral Research, Department of Orthodontics, School and Hospital of Stomatology, Shandong University, Shandong University, Wenhua West Road 44-1, 250012 Jinan, China

multiple myeloma, and periodontitis (McInnes et al. 2016; Nishimoto and Kishimoto 2006). In response to exogenous infections or autologous antigens, IL-6 is released from leukocytes, fibroblasts, keratinocytes and stromal cells (Kim et al. 2015). The increased level of IL-6 in local tissue trigger osteoclast formation, resulting in bone destruction.

Previous evidences have indicated that IL-6 has no significantly direct effect on osteoclasts formation, the promotive effect of IL-6 on osteoclasts formation is predominantly considered to achieved by indirectly inducing production of receptor activator for nuclear factor-κ B ligand (RANKL), the key stimulator for osteoclastic differentiation, by osteoblastic/stromal cells (Lindberg et al. 2001; Palmqvist et al. 2002). However, recent studies suggest that IL-6 directly inhibits, rather than stimulates osteoclasts formation (Duplomb et al. 2008; Yoshitake et al. 2008). Thus, the precise role of IL-6 in inflammatory bone resorption remains controversial.

For signaling, IL-6 binds to IL-6 receptor (IL-6R) promotes homodimerization of signal-transducing co-receptor glycoprotein 130 (gp130) and therefore activates downstream signaling pathways such as Janus-kinases/signal transducers and activators of transcription (Jak/STAT), phosphatidylinositol 3-kinase (PI3K) and mitogen-activated protein kinase (MAPK) cascades (Rose-John 2017). As IL-6R exists in membrane-bound as well as soluble forms, IL-6 signaling is classified as two distinct pathways. Binding of IL-6 to membrane-bound IL-6R expressed predominantly in hepatocytes and certain subpopulations of immune cells activates classical signaling which is responsible for acute-phase response and mediates anti-inflammatory effects (Heinrich et al. 1998). However, because gp130 is ubiquitously expressed in almost all cells of the body, IL-6 also can induce trans-signaling cascades through binding to soluble IL-6R (sIL-6R) in other types of cells which don't express membrane-bound IL-6R. IL-6 trans-signaling via sIL-6R mainly accounts for the pro-inflammatory reactions and cancer development (Rose-John and Neurath 2004; Rose-John et al. 2006). A soluble form of gp130 (sgp130) has been shown to specifically inhibit IL-6 trans-signaling whereas leaving IL-6 classic signaling unaffected (Garbers et al. 2015; Jostock et al. 2001). Thus, sgp130 is considered to be a natural antagonist of IL-6 trans-signaling, probably to prevent inflammatory responses in a variety of chronic and autoimmune diseases (Rose-John 2017).

Mature giant multinucleated osteoclasts are derived from bone marrow monocytes (BMMs) which express IL-6R in the membrane (Audet et al. 2001; Peters et al. 1997, 1998). This allows the activations of both IL-6 classical signaling and trans-signaling in BMMs. Our previous study demonstrated that IL-6 in the combination of sIL-6R significantly promoted low level of RANKL-induced osteoclast differentiation which was not affected by IL-6 alone (Feng et al. 2017). These observations lead us to propose that sIL-6R-mediated trans-signaling pathway plays a decisive role in this positive regulation on osteoclast differentiation. In the present study, we aimed to validate the above assumptions using sgp130 to block IL-6 trans-signaling pathway in mouse BMMs.

Materials and methods

Cell culture and antibodies

The α-minimum essential medium (α-MEM), penicillin/streptomycin and fetal bovine serum (FBS) were purchased from Gibco-BRL (Gaithersburg, MD, USA). Cell Counting Kit-8 (CCK-8) was purchased from DOJINDO Laboratories (Dojindo Laboratories, Tokyo, Japan). Recombinant soluble mice RANKL, macrophage colony-stimulating factor (M-CSF), murine IL-6, soluble murine IL-6R and sgp130 were purchased from R&D System (Minneapolis, MN, USA). Specific antibodies against phospho-STAT3 (Tyr705), extracellular signal-regulated kinase (ERK), c-Jun N-terminal kinase (JNK), anti-STAT3, p38, nuclear factor kappa light chain enhancer of activated B cells (NF-κB), phospho-ERK, phospho-JNK, phospho-p38, phospho-NF-κB were obtained from Cell Signaling Technology (Cambridge, MA, USA). Anti-nuclear factor of activated T cells cytoplasmic 1 (NFATc1), anti-c-fos, anti-TNF receptor associated factor-6 (TRAF-6) and anti-β-actin antibodies were obtained from Abcam (Cambridge, MA, USA).

Mouse bone marrow macrophage preparation and osteoclastic differentiation

The animal care and experimental protocol were approved by a committee of the Medical Ethics Committee for Experimental Animals, Shandong University School of Stomatology (No. 20,210,118). Male, four to six-week-old C57BL/6 mice were used in this study. Primary bone marrow macrophages (BMMs) were isolated from the whole bone marrow as described previously. Briefly, mice were sacrificed by decapitation under deep anesthesia with 10% Chloral hydrate. Tibiae and femurs were isolated and flushed with α-MEM. The cells were cultured in α-MEM containing 10% FBS, 100 U/ml penicillin G, and 100 μ g/ml streptomycin at 37 °C under 5% CO_2. Non-adherent cells were layered onto a Ficoll density gradient solution and centrifuged at 440 g for 30 min at room temperature. Cells lying in the upper layer were harvested as BMMs. The cells were seeded in 6-well plate (5×10^5 cells/well) or 24-well plates (3×10^4 cells/well) and cultured for 6 days in α-MEM supplemented with

10% FBS, 30 ng/ml M-CSF and 10 or 50 ng/ml RANKL in the absence or presence of given concentrations of IL-6, sIL-6R and sgp130. The culture medium was changed to fresh medium every other day.

Proliferation assays

Cell proliferation activity was evaluated using CCK-8 Assay Kit (Beyotime) following the manufacturer's protocol. Mouse BMMs were seeded onto 96-well plates at a final concentration of 5×10^3 and cultured for 3 days as indicated with the cytokines and cytokine receptors. After incubating for 0, 24, 48 and 72 h, CCK-8 solution was added to each well and then incubated for 1 h. Optical density (OD) values at the wavelength of 450 nm were measured with a microplate reader (Bio-Rad Laboratories Inc., Hercules, CA, USA). All of the values were measured in triplicate per experiment.

Tartrate-resistant Acid phosphatase (TRAP) staining

TRAP staining was used to verify osteoclasts formation. Mouse BMMs were seeded onto 24-well plates at a density of 3×10^4 and cultured in α-MEM supplemented with stimulus as indicated for 4 days. Cells were fixed with 4% formaldehyde for at least 15 min at room temperature and stained for TRAP using TRAP-staining solution: 0.1 M sodium acetate (pH 5.0) containing 0.01% naphthol AS-MX phosphate (Sigma-Aldrich) as a substrate, and 0.03% red violet LB salt (Sigma-Aldrich) as a stain for the reaction product in the presence of 50 mM sodium tartrate. Cell nucleus were counterstained with hematoxylin for 2 min. Multinucleated TRAP-positive cells with at least 3 nuclei were scored as osteoclasts.

Resorption pit formation assay

Pit formation assay was performed using the Corning Osteo Assay Surface Multiple Well Plate (Corning, Inc., Corning, NY, USA). BMMs were seeded onto 96-well plates at a density of 5×10^3 and cultured in α-MEM supplemented with stimulus as indicated for 14 days. The culture medium was replaced with fresh medium containing these reagents every 2 days. After the culture, plates were stained with Von Kossa to increase contrast between pits and surface coating and observed under a light microscope. The percentage of the resorbed areas and the number of resorption pits in three random resorption sites were measured under microscopic examination using Image-Pro Plus 6.2 software (Media Cybernetics, Silver Spring, MD, USA). The assays were performed in triplicate, and a representative view from each assay is presented.

RNA extraction and real-time RT-PCR analysis

BMMs were seeded in 24-well plates (3×10^4 cells/ well) and incubated with stimulus as indicated for 2 days. Total RNA was isolated from cells using a RNeasy Mini kit (Qiagen, Valencia, CA, USA), quantitative real-time PCR analysis was performed to detect mRNA expression of TRAP, Cathepsin K (CK), Calcitonin receptor (CTR) and matrix metalloproteinase (MMP)-9 using the primer sequences shown in Table 1. All quantitative reverse transcription-PCRs were performed using Roche LightCycler 480 Real-Time PCR system (Roche, Sussex, UK), and all samples were run in triplicate. The cycling conditions were as follows: 40 cycles of 95 °C for 3 s and 60 °C for 30 s. Relative quantities of the tested genes were normalized to GAPDH mRNA. Analysis of the relative quantitation required calculations based on the threshold cycle, i.e., the cycle number at which the amplification plot crosses a fixed threshold above the baseline (Ct). Relative quantitation was performed using the comparative $\Delta\Delta$ Ct method according to the manufacturer's instructions.

Co-immunoprecipitation assay.

BMMs were plated in six-well plates at a density of 2×10^5 cells/well. When the cells grew to confluent, they were pretreated with or without IL-6/sIL-6R (200/50 ng/ml, 9.2/0.97 nM) with/without sgp 130 (100 ng/ml, 1 nM) for 4 h. The cells were then stimulated with 10 ng/ml RANKL for 0, 5, 15 or 30 min and then subjected to co-immunoprecipitation assay using Immunoprecipitation (IP) Kit (Proteintech Group, Chicago, USA) according to the manufacturer's instructions. Briefly, cells were washed three times with ice-cold phosphate-buffered saline and lysed in IP lysis buffer. Cell debris was removed by centrifugation at 10,000 rpm

Table 1 Oligonucleotide primers used for real-time PCR

Gene name		Oligonucleotide Sequence (5′ → 3′)
IL-1β	Forward	ACAGATGAAGTGCTCCTTCCA
	Reverse	GTCGGAGATTCGTAGCTGGAT
TNFα	Forward	CCCAGGGACCTCTCTCTAATC
	Reverse	ATGGGCTACAGGCTTGTCACT
IFNγ	Forward	CTAATTATTCGGTAACTGACTTGA
	Reverse	ACAGTTCAGCCATCACTTGGA
TRAP	Forward	ACACAGTGATGCTGTGTGGCAACTC
	Reverse	CCAGAGGCTTCCACATATATGATGG
Cathepsin K	Forward	AGGCGGCTATATGACCACTG
	Reverse	CCGAGCCAAGAGAGCATATC
Calcitonin receptor	Forward	ACCGACGAGCAACGCCTACGC
	Reverse	GCCTTCACAGCCTTCAGGTAC
MMP-9	Forward	CGTCGTGATCCCCACTTACT
	Reverse	AGAGTACTGCTTGCCCAGGA
GAPDH	Forward	TGGCCTTCCGTGTTCCTAC
	Reverse	GAGTTGCTGTTGAAGTCGCA

for 15 min at 4 °C. After that, cell lysates were incubated with anti-RANK antibody at 4 °C for overnight and rotated with protein A sepharose beads slurry at 4 °C for 4 h. Then, the beads were washed three times with washing buffer. The immunoprecipitates or whole-cell lysates were subjected to sodium dodecyl sulfate-polyacrylamide gel electrophoresis (SDS-PAGE) and transferred to Immobilon polyvinylidene difluoride membranes (Millopore Corporation, Billerica, MA, USA). The membranes were immunoblotted with rabbit anti-TRAF6 for 1 h at room temperature followed by horseradish peroxidase-conjugated goat anti-rabbit IgG and visualized by the ECL system (SmartChemi 420; Sagecreation, Beijing, China).

Western blot analysis

BMMs were seeded in six-well plates at a density of 1×10^5 cells/well and cultured with stimulus as indicated. After 2 days, the total protein was collected for NFATc1 and c-fos immunoblotting. To evaluate the influence of IL-6, sIL-6R and sgp130 on the phosphorylation of STAT3, BMMs were seeded in six-well plates at a density of 1×10^5 cells/well and cultured with stimulus as indicated for 48 h and cell lysates were collected for p-STAT3/STAT3 immunoblotting. To detect the effect of IL-6/sIL-6R/sgp130 on RANKL-activated intracellular signal transduction cascades, BMMs were seeded in six-well plates at a density of 1×10^5 cells/well. When the cells were confluent, they were pre-treated with or without IL-6/sIL-6R (200/50 ng/ml) and/or sgp130 (100 ng/ml) for 4 h. The cells were then stimulated with
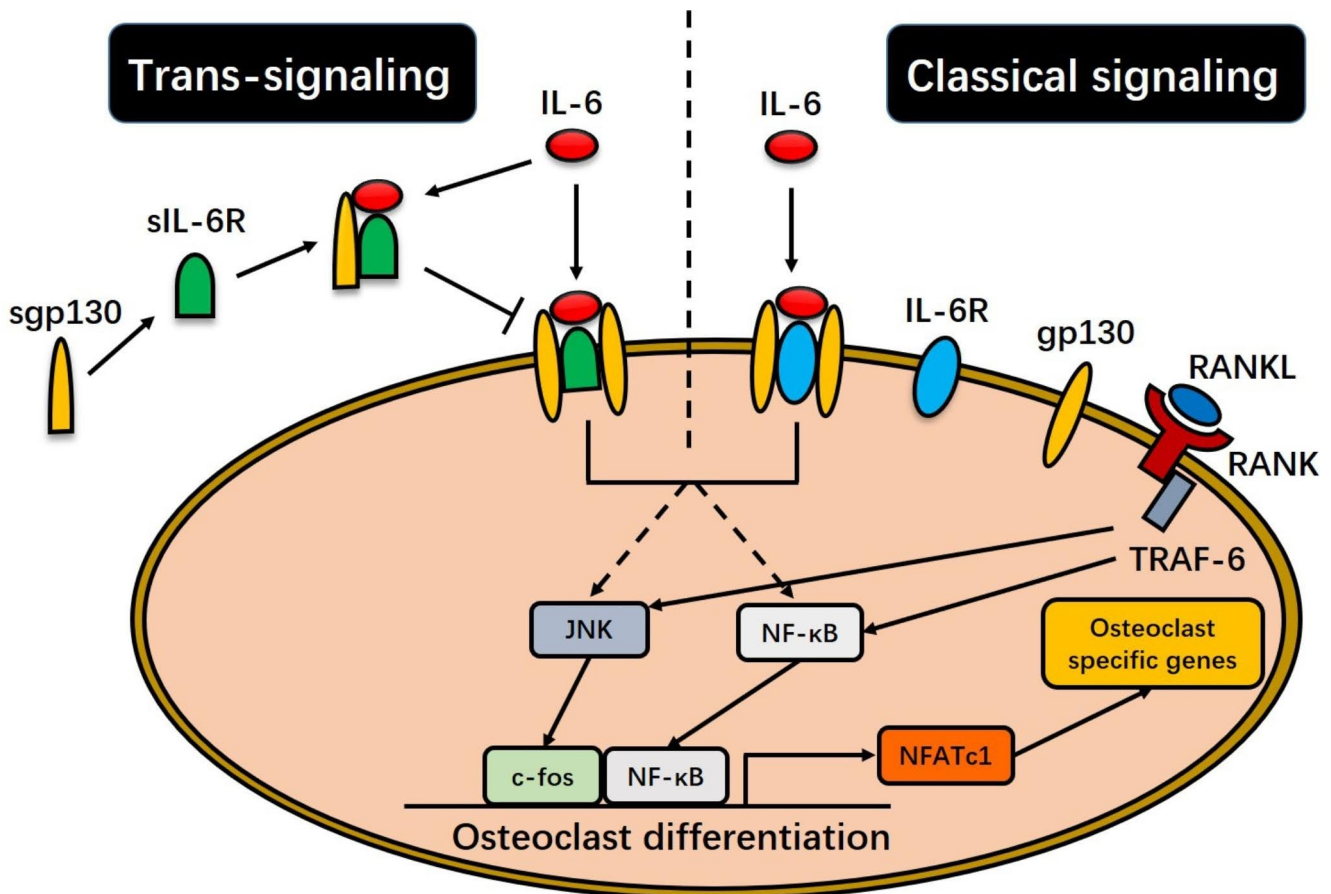
Fig. 1 *sIL-6 activates IL-6 trans-signaling and promotes low concentration of RANKL-induced osteoclastic differentiation by mouse BMMs* BMMs were cultured in the presence of different concentrations of RANKL (0–50 ng/ml) with or without gradient concentration of IL-6 (0-200 ng/ml) and sIL-6R (0-100ng/ml). After 4 days' culture, TRAP staining was performed to visualize mature osteoclasts followed by cell count. The evaluation of phosphorylation on tyrosine 705 in STAT3 and the expression of several key inflammatory factors was used to determine the activation of IL-6 signaling pathway. (**a**) Western blot for global tyrosine phosphorylation at position 705 of STAT3 and qRT-PCR for IL-6-induced transcriptional activation of inflammatory factors. (**b**) Representative images of TRAP staining for BMMs (original magnification, × 200) and statistical analysis for the number and mean size of TRAP positive multinucleated cells. The data are representative of three independent experiments expressed as means ± SD. Different letters above bars indicate significant differences between groups (a < b < c < d, $p < 0.05$)

10 ng/ml RANKL for 0, 15, 30 or 60 min. After that, cell lysates were prepared with RIPA lysis buffer (Beyotime, Beijing, China). Cell debris was removed by centrifugation at 10,000 rpm for 15 min at 4 °C followed by protein concentration measurement using the BCA method. Protein was denatured by boiling for 5 min before electrophoresis. Each protein sample was subjected to 6% SDS–PAGE, and transferred to immobilon polyvinylidene difluoride membranes. The membranes were blocked with 5% BSA in TBS-T for 1 h, and incubated with rabbit anti-NFATc1, anti-c-fos, anti-phospho-STAT3, anti-STAT3, anti-phospho-p38, anti-p38, anti-phospho-ERK, anti-ERK, anti-phospho-JNK, anti-JNK, anti-phospho-NF-κB and anti-NF-κB antibodies for 1 h at room temperature. The membranes were then washed three times with TBS-T for 5 min each and incubated with horseradish peroxidase-conjugated goat anti-rabbit IgG at a dilution of 1:1000. After three washes with TBS-T, the immunoreactive bands were visualized with ECL detection system. β-actin serves as loading control.

Statistical analysis

The data are expressed as means ± standard deviations (SD) calculated from at least three independent experiments. SPSS 21.0 software (SPSS, Inc., Chicago.IL) was used for data analysis. One-way ANOVA was used for multiple groups' comparison, and the mean value of each group was compared using the Student-Newman-Keuls (SNK) test. $P < 0.05$ was considered statistically significant.

Results

Activation of IL-6 trans-signaling enhances IL-6 signaling cascades and promotes low concentration of RANKL-induced osteoclastic differentiation by mouse BMMs.

STAT3 phosphorylation is a key event in IL-6 signaling cascades. Here, we evaluated the phosphorylation on tyrosine 705 in STAT3 by Western blot to determine the activation of IL-6 signaling pathway. As revealed in Fig. 1a, the level of STAT3 phosphorylation was gradually increased with the concentration of IL-6 and attained a maximal level when IL-6 concentration was raised to 100 ng/ml.
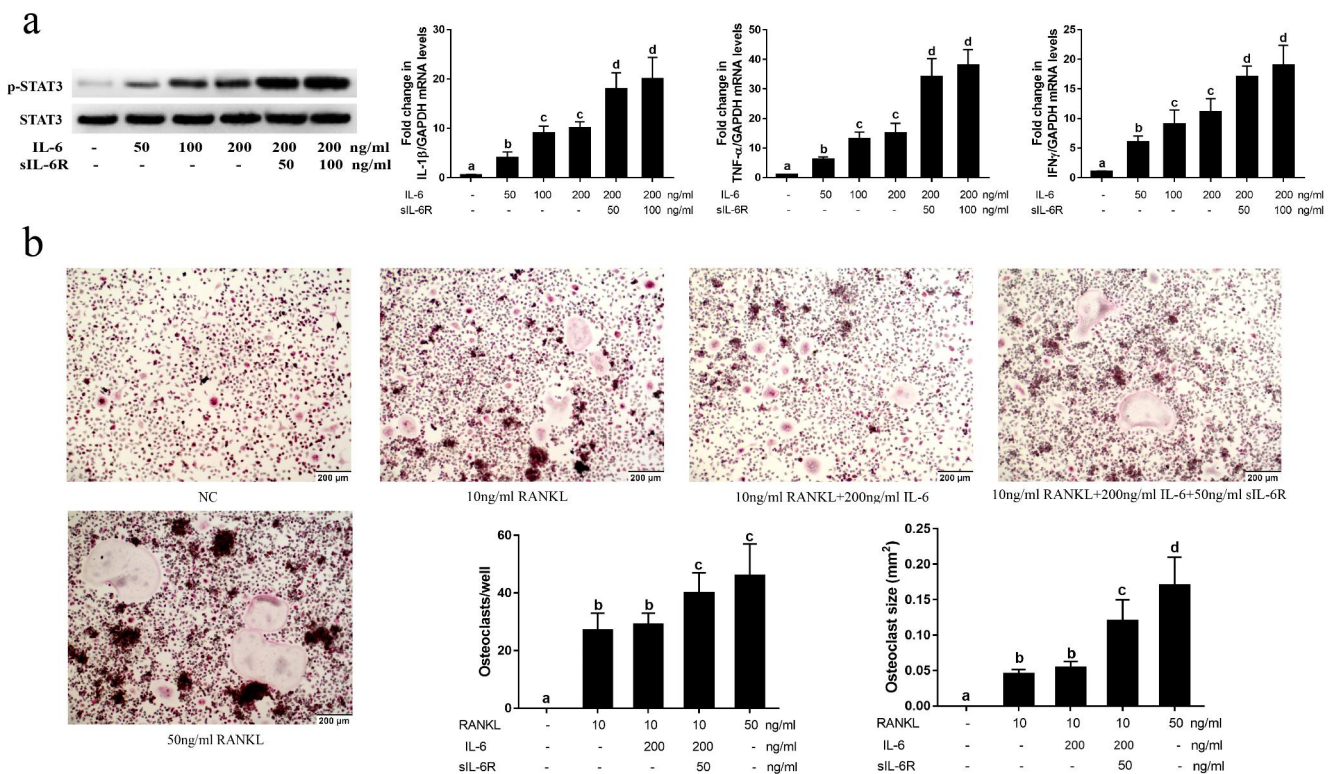
Fig. 2 *Sgp130 inhibits IL-6 trans-signaling in mouse BMMs*
(**a**) BMMs were cultured in the presence of different concentrations of IL-6 (0-200 ng/ml), sIL-6R (0-100 ng/ml) and/or sgp130 (0-200 ng/ml) for 48 h. Cell lysates were collected for analysis of global tyrosine phosphorylation at position 705 of STAT3. (**b**) BMMs seeded in 96-well plates were treated with or without IL-6, sIL-6R and sgp130 as indicated. After incubation for 0, 24, 48 and 72 h, CCK8 assay was performed to determine cell proliferation. (**c**) Total RNA was isolated and qRT-PCR was performed for IL-6-induced transcriptional activation of inflammatory factors. Different letters above bars indicate significant differences between groups (a < b < c, $p < 0.05$)

Doubling IL-6 concentration to 200 ng/ml didn't yield more STAT3 phosphorylation. Strikingly, addition of sIL-6R further heightened STAT3 phosphorylation based on adequate amounts of IL-6. The same result was observed in the expression of several key inflammatory factors associated with IL-6 signaling pathway activation such as IL-1β, TNF-α and IFNγ.

Based on the data from our previous studies, compared with the large quantity of giant TRAP-positive multinucleated giant cells induced by 50 ng/ml RANKL, whereas 10 ng/ml RANKL was only able to induce a small number of osteoclasts with smaller size. Therefore, we designated 10 ng/ml as a low level of RANKL concentration in this study. As shown in Figs. 1b and 10 ng/ml RANKL treatment of BMMs bring forth a few TRAP-positive osteoclasts with smaller number and size in comparison with those from 50 ng/ml RANKL group. Addition of 200 ng/ml IL-6 had no influence on 10 ng/ml RANKL-induced osteoclastogenensis. However, when 200 ng/ml IL-6 was used in combination with 50 ng/ml sIL-6R, the osteoclastogenesis induced by 10 ng/ml RANKL was strongly enhanced, as evidenced by the both increased number and size of TRAP-positive osteoclasts.

These results indicated that activation of IL-6 trans-signaling pathway by sIL-6R strengthens IL-6 signaling cascades and promotes low level of RANKL-induced osteoclasts formation by BMMs.

Sgp130 inhibits IL-6 trans-signaling in mouse BMMs

As an antagonist of IL-6 trans-signaling, recombinant sgp130 binds to IL-6/sIL-6R complex in competition with membrane-bound gp130 to block IL-6 trans-signaling pathway. As shown in Figs. 2a and 50 ng/ml sIL-6 significantly increased the STAT3 phosphorylation induced by 200 ng/ml IL-6. 100 ng/ml sgp130 suppressed the phosphorylation of STAT3 to the level of 200 ng/ml IL-6 treated group. Increasing the concentration of sIL-6R and sgp130 to 100 ng/ml further reduced STAT3 phosphorylation which was not changed by enhancing the concentration of sgp130 to 200 ng/ml, which indicates that sgp130 can trap IL-6 in IL-6-sIL-6R complex and the antagonistic ability of sgp130 on IL-6 signaling is dependent on the amount of sIL-6R.

Activation of IL-6 signaling has been reported to regulate cell proliferation and differentiation of monocytes (Chomarat et al. 2000; Dixit et al. 2018). Using CCK8 assay, we found that sIL-6 significantly promoted cell proliferation induced by IL-6 treatment, whereas sgp130 inhibited colony formation of mouse BMMs to the level of IL-6 treated group (Fig. 2b).
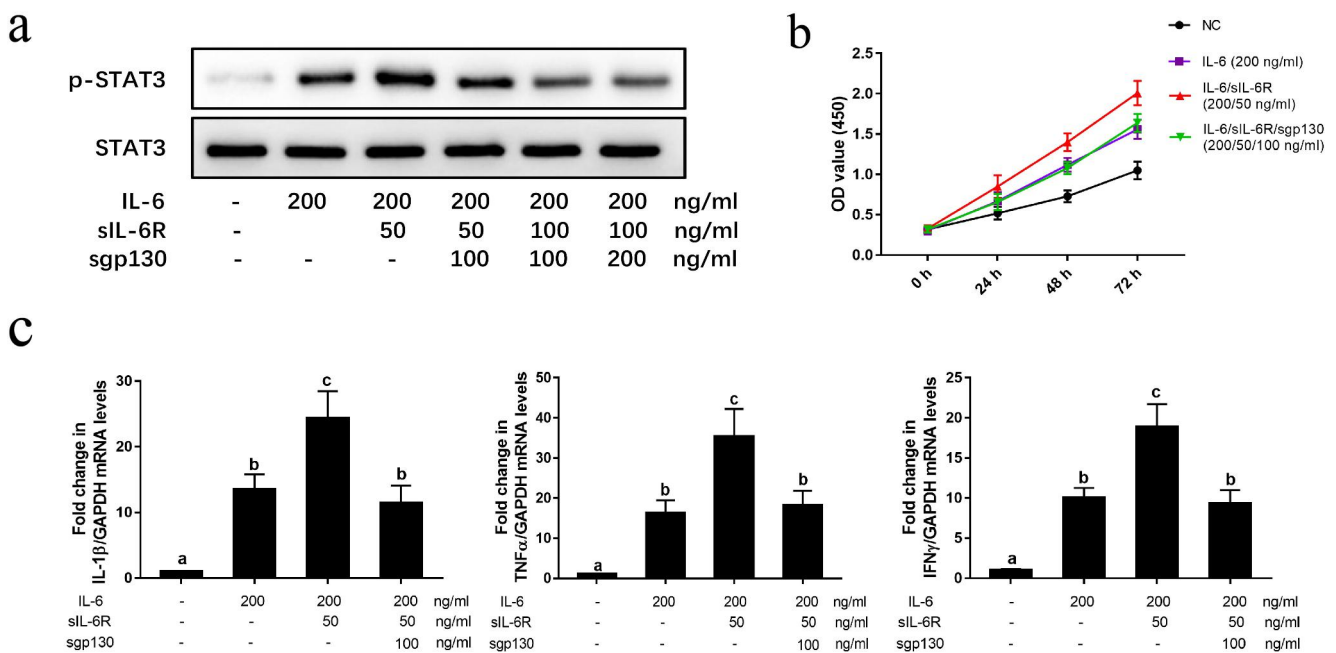
Fig. 3 *sgp130 abrogates the promotive effect of IL-6/sIL-6R on low concentration of RANKL-induced osteoclasts formation and bone resorption by mouse BMMs*

BMMs were cultured in the presence of 10 ng/ml RANKL with or without IL-6/sIL-6R (200/50 ng/ml) and/or sgp130 (50 ng/ml). After 4 days' culture, TRAP staining was performed to visualize mature osteoclasts followed by cell count. On day 14, cells were removed and the mineral-coated wells were counterstained by Von Kossa stain. Resorption pits were examined by light microscope. (**a**) Representative images of TRAP staining for BMMs (original magnification, × 200) and statistical analysis for the number and mean size of TRAP positive multinucleated cells. (**b**) Representative images of resorption pits after Von Kossa staining (original magnification, × 200) and statistical analysis for the number and area of resorption pits. The data are expressed as means ± SD. Different letters above bars indicate significant differences between groups (a < b < c,

Similar observations were made for the expression of key inflammatory factors including IL-1β, TNF-α and IFNγ that sgp130 abrogated the increase of these factors induces by addition of sIL-6R into IL-6 (Fig. 2c). These results confirmed the effectiveness of sgp130 in blocking IL-6 trans-signaling pathway.

Blockage of IL-6 trans-signaling abrogates the promotive effect of IL-6/sIL-6R on low concentration of RANKL-induced osteoclasts formation and bone resorption by mouse BMMs.

As mentioned above, IL-6 in combination with sIL-6R significantly increased low level of RANKL-induced osteoclasts formation. When 100 ng/ml sgp130 was applied to RANKL/IL-6/sIL-6R culture system, the number and size of TRAP-positive osteoclasts were both decreased into the level of 10 ng/ml RANKL-treated group (Fig. 3a).

Besides typical morphological features such as TRAP-positive multinucleated giant cell body, bone resorption activity is another principal character of mature osteoclasts. In this study, we employed pit formation assay to determine the effect of recombinant sgp130 on bone resorptive activity of low level of RANKL-induced osteoclasts in the presence of IL-6/sIL-6R. As is shown in Fig. 3b, few clear resorption pits were observed in the culture treated with 10 ng/ml RANKL. Cotreatment with IL-6 and sIL-6R resulted in remarkably enlarged number and area of resorption by the BMMs induced by low level of RANKL. However, addition of sgp130 to RANKL/IL-6/sIL-6R culture system generated a significant decrease in the number and area of resorption pits to the level of 10 ng/ml RANKL-treated group. Taken together, these results clearly demonstrated that blockage of IL-6 trans-signaling by sgp130 prohibits the promotive effect of IL-6/sIL-6R on low level of RANKL-induced osteoclasts formation and resorptive ability.

Blockage of IL-6 trans-signaling abrogates the promotive effect of IL-6/sIL-6R on expressions of osteoclast-specific genes and activation of osteoclastic differentiation-related signaling pathways induced by low concentration of RANKL in mouse BMMs.

The binding of RANKL to its receptor RANK recruits adaptor molecule TRAF6 which then activate MAPKs, nuclear factor-κB (NF-κB) pathway, and finally amplify NFATc1 and c-fos activation for the transcription of osteoclastic marker genes including TRAP, MMP-9, cathepsin K and CTR. We first sought to determine whether blocking IL-6 trans-signaling pathway altered recruitment of TRAF6 by RANKL-RANK binding. As shown in Fig. 4c, immunoprecipitation assay revealed that the association of TRAF6 with RANK peaked at 5 min after 10 ng/ml RANKL treatment and declined thereafter. Pretreatment with IL-6/sIL-6R (200/50 ng/ml) and/or 100 ng/ml sgp130 didn't change the association of TRAF6 with RANK in response to RANKL stimulation.

NFATc1 and c-fos are among the most crucial transcriptional factors in osteoclastic differentiation by BMMs. Western blotting revealed that the protein expressions of NFATc1 and c-fos were induced by 10 ng/ml RANKL. Additional treatment with IL-6/sIL-6R (200/50 ng/ml) significantly potentiated the synthesis of both proteins. When 100 ng/ml sgp130 was used to inhibit IL-6 trans-signaling, the protein expressions of NFATc1 and c-fos were lowered to the level of 10 ng/ml RANKL treated group (Fig. 4a).

Recruitment of TRAF6 to RANK activates NF-κB, MAPKs, initiating transcription of osteoclast specific factors in osteoclast precursors. We next confirmed whether blocking IL-6 trans-signaling affects the activation of osteoclastic differentiation-associated signaling pathways. As evidenced by the immunoblot assay in Fig. 4d, NF-κB phosphorylation was significantly induced in mouse BMMs by 10 ng/ml RANKL. Pretreatment of BMMs with IL-6/sIL-6R (200/50 ng/ml) strongly potentiated NF-κB phosphorylation. However, when the cells were pretreated with IL-6/sIL-6R (200/50 ng/ml) in the combination of 100 ng/ml sgp130, the phosphorylation of NF-κB was suppressed to the level of 10 ng/ml RANKL treated group. With respect to MAPKs signaling pathways, p38 phosphorylation induced by RANKL was not changed by IL-6/sIL-6R and sgp130. Notably, Low level of RANKL-induced phosphorylation of ERK and JNK was enhanced by IL-6/sIL-6R and declined when sgp130 was concomitantly added.

We next confirmed the effect of blocking IL-6 trans-signaling on the promotion of low concentration of RANKL-induced osteoclastogenensis by osteoclastic marker genes and critical transcriptional factors. After 2 days of osteoclastic induction, the mRNA expression levels of osteoclast-specific factors including TRAP, MMP-9, cathepsin K and CTR were remarkably increased in the presence of low level of RANKL. Addition of IL-6/sIL-6R (200/50 ng/ml) further enhanced the mRNA expression of these osteoclast-specific factors, which were then strongly suppressed by blocking IL-6 trans-signaling with 100 ng/ml sgp130 (Fig. 4b).

These results further indicate that blocking IL-6 trans-signaling by sgp130 inhibits the promotive effect of IL-6/sIL-6R on low level of RANKL-induced osteoclastic differentiation at transcription level (schematically summarized in Fig. 5).

Discussion

It's well known that IL-6 trans-signaling mediates pro-inflammatory effects in immune response and has been used as a therapeutic target for autoimmune disease. In the
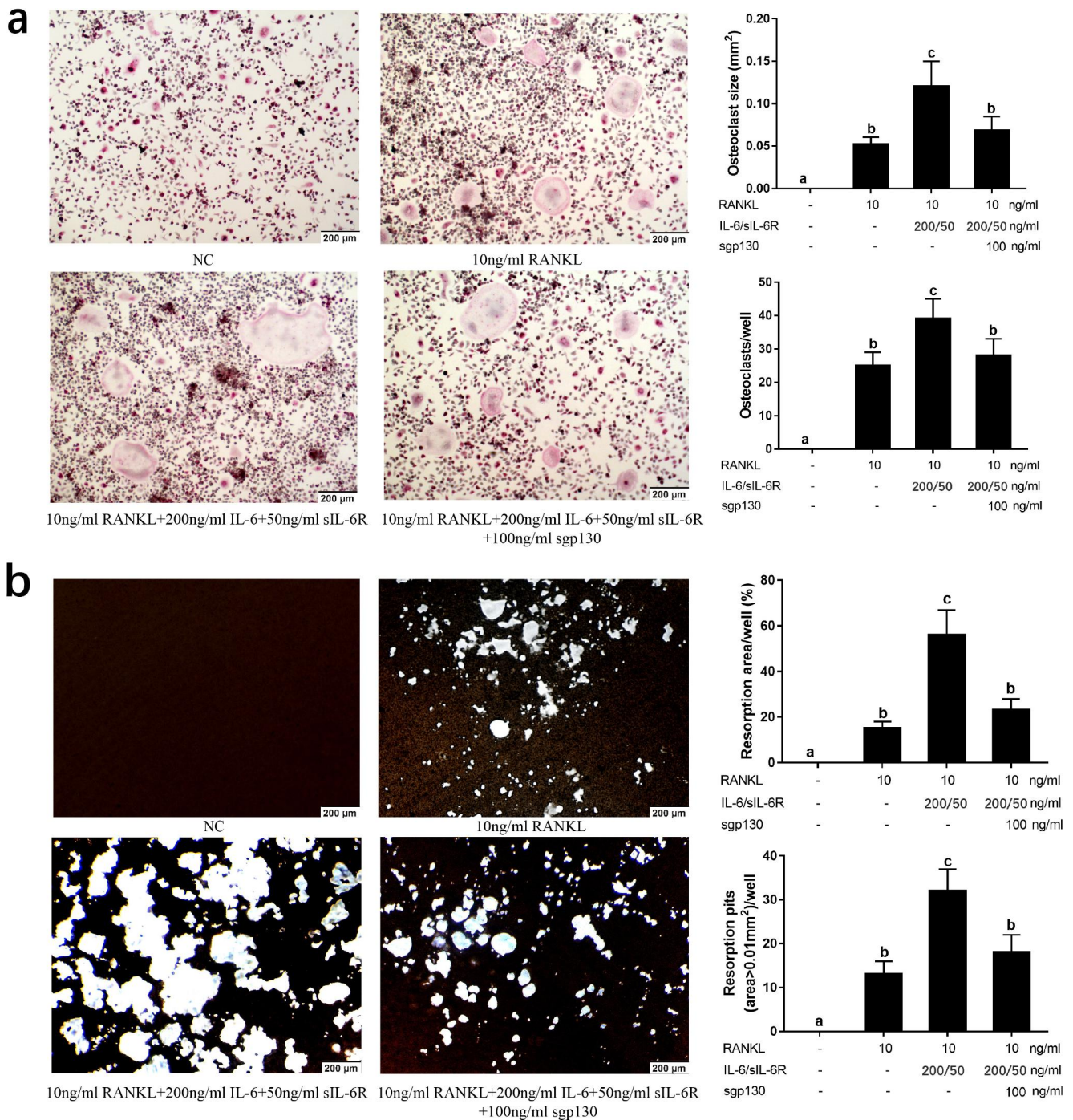
Fig. 4 *sgp130 abrogates the promotive effect of IL-6/sIL-6R on expressions of osteoclast-specific genes and activation of osteoclastic differentiation-related signaling pathways induced by low concentration of RANKL in mouse BMMs*

(**a**) BMMs were cultured in the presence of 10 ng/ml RANKL with or without IL-6/sIL-6R (200/50 ng/ml) and/or sgp130 (100 ng/ml) for 2 days. After that, the total protein of cell lysates was subjected to SDS-PAGE, followed by Western blotting with antibodies specific to NFATc1 and c-fos. β-actin was used as a loading control. (**b**) The total RNA was extracted and subjected to qRT-PCRs using probes specific for TRAP, cathepsin K, MMP-9 and CTR. The levels of osteoclast specific genes mRNA expression were normalized to GAPDH expression. (**c**) BMMs cells were pretreated with IL-6/sIL-6R (200/50 ng/ml) in the presence or absence of 100 ng/ml sgp130 for 4 h followed by 10 ng/ml RANKL treatment for the indicated times. Cell lysates were immunoprecipitated with anti-RANK antibody and coprecipitated TRAF6 was detected by immunoblotting with anti-TRAF6 antibody. Total cell lysate content of TRAF6 were determined by immunoblot. (**d**) BMMs cells were pretreated with or without IL-6/sIL-6R (200/50 ng/ml) in the presence or absence of 100 ng/ml sgp130 for 4 h followed by 10 ng/ml RANKL treatment. Cell lysates were collected at the indicated time points and subjected to Western blot analysis with specific antibodies against p-38, phosphor-p-38, JNK, phosphor-JNK, ERK, phosphor-ERK, NF-κB, phosphor-NF-κB to determine the level of phosphorylation of indicated signaling molecules. The data are expressed as means ± SD. Different letters above bars indicate significant differences between groups (a < b < c, $p < 0.05$)
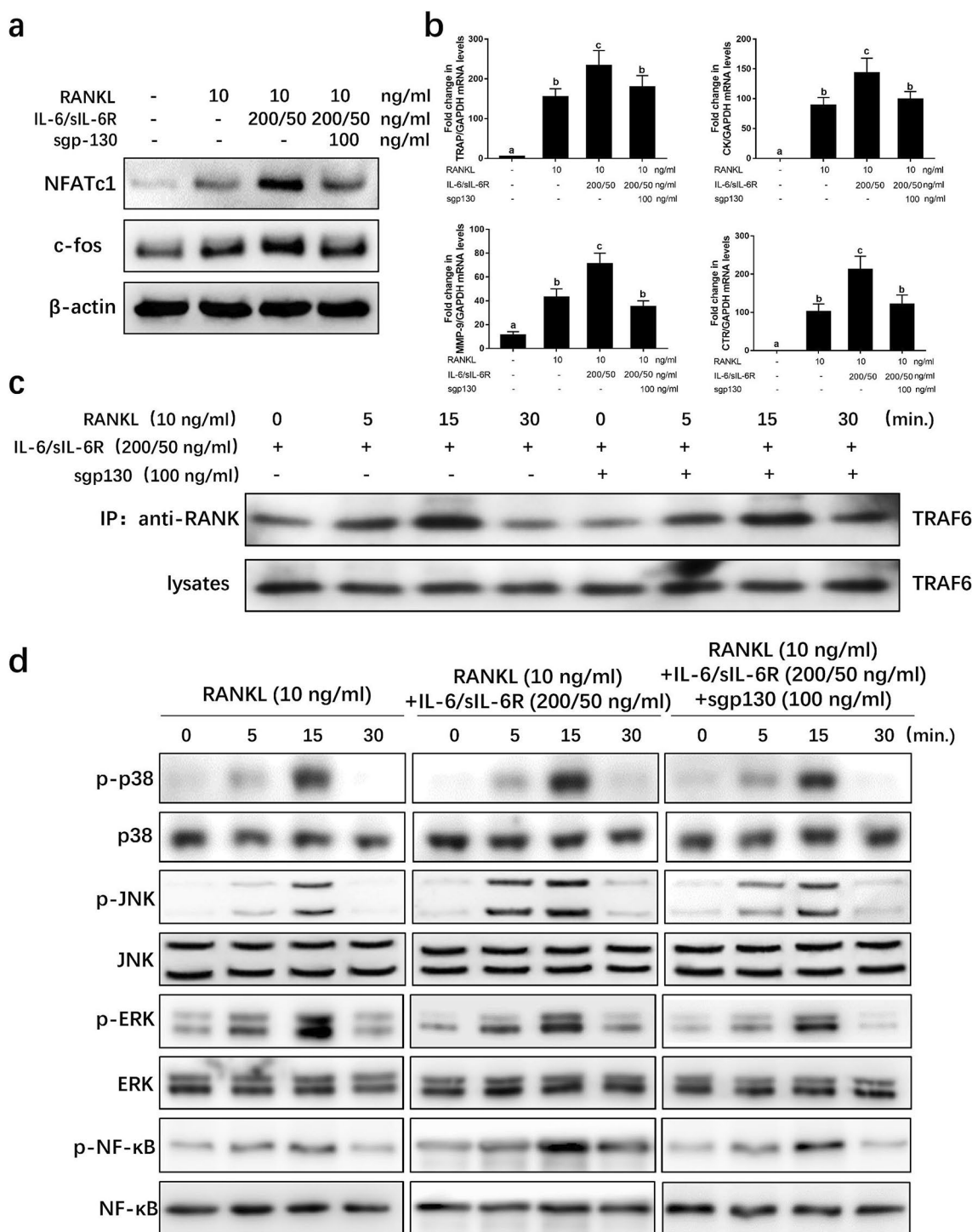
Fig. 5 *Schematic diagram of IL-6 classic, trans-signaling and their cross-talk with RANK-RANKL signaling responsible for osteoclastic differentiation*

 The process that IL-6 binds to membrane-bound IL-6R resulting in dimerization of gp130 and activation of downstream signaling cascades is termed classic signaling. While in trans-signaling, IL-6 binds to sIL-6R and then activates gp130 expressed on cell membrane. Sgp130 can trap IL-6-sIL-6R complex thus blocking IL-6 trans-signaling. IL-6 classic signaling alone has no effect on RANKL-induced osteoclast formation. The presence of sIL-6R enables coactivation of IL-6 classic and trans-signaling, which enhances expressions of osteoclastic transcriptional factors including NFATc1, c-fos and osteoclast specific genes via cross-talk with NF-κB and JNK signaling pathways, thus leading to potentiation of RANKL-induced osteoclastic differentiation. Sgp130 inhibits this activation process through inhibiting IL-6 trans-signaling

present study, we demonstrate that blocking IL-6 trans-signaling recombinant mouse sgp130 abrogates the promotive effect of IL-6/sIL-6R on low level of RANKL-induced osteoclasts formation and bone resorption by mouse BMMs at transcription level. Our findings distinguish the unique role of IL-6 trans-signaling from its classic signaling in direct mediation of bone resorption and provides evidences for the bone reserving role of selective inhibition of IL-6 trans-signaling other than anti-inflammatory effects.

There are long-running disputes over the effect of IL-6 on osteoclast formation. Earlier studies have shown that IL-6 indirectly promote osteoclast formation by inducing RANKL by osteoclast-supporting cells (Liu et al. 2005; Wong et al. 2006). Recent studies have revealed that IL-6R is expressed in osteoclast precursors and thus IL-6 can directly act on osteoclast precursors to regulate their osteoclastic differentiation (Kudo et al. 2003; Ohsaki et al. 1992), although with both promotive and inhibitive effects being reported (Axmann et al. 2009; Duplomb et al. 2008; Kudo et al. 2003; Yoshitake et al. 2008). Our previous study indicated that IL-6 in the presence of sIL-6R exhibits distinct effects on osteoclast formation depends on the level of RANKL used in osteoclastic induction culture system (Feng et al. 2017). In the present study, we replicated the finding of above research that IL-6/sIL-6R promote low level of RANKL-induced osteoclasts formation. Based on the finding, it is postulated that in the initial stage of inflammatory response, when the level of RANKL is relatively low, IL-6/sIL-6R released by local active immune cells promotes osteoclasts formation and bone resorption, while in the progressive stage, when the level of RANKL rises sharply, IL-6/sIL-6R may serve to protect the bone from over-resorption by suppressing RANKL-induced osteoclasts formation (Feng et al. 2017).

Osteoclast are specialized cells for bone resorption which are derived from the monocyte/macrophage hematopoietic lineage. As IL-6R has been found to be expressed in the membrane of monocytes/macrophages, both IL-6 classic signaling and trans-signaling are present in osteoclasts and their precursors (Audet et al. 2001; Peters et al. 1997, 1998). The founding of our previous study that combined use of IL-6 and sIL-6R significantly promoted low level of RANKL-induced osteoclast differentiation which was not affected by IL-6 alone indicates that IL-6 classic signaling alone is not enough to exert impact on osteoclastic differentiation unless sIL-6-mediated IL-6 trans-signaling is activated simultaneously. Consistent with our results, several lines of evidence have also suggested that sIL-6 strongly sensitizes target cells such as hematopoietic progenitors which are only responsive to IL-6 in the presence of sIL-6R (Jones 2005; Rose-John 2006).

The fact that treatment of mouse BMMs with 200 ng/ml IL-6 resulted in activation of IL-6 signaling identical to that induced by 100 ng/ml IL-6 suggests 100 ng/ml IL-6 is sufficient to saturate the binding sites of membrane-bound IL-6R and therefore we chose 200 ng/ml as final concentration in order to leave adequate free IL-6 for sIL-6R-mediated trans-signaling. Phosphorylation analysis of STAT3 revealed that IL-6-induced activation of IL-6 signaling in mouse BMMs expressing membrane-bound IL-6R was significantly enhanced by the addition of sIL-6R, indicating that both classic and trans-signaling pathways can act in parallel and the classic signaling can also be inhibited in the presence of sufficient sIL-6R and sgp130, which is in concordance with the reports from Garbers, C. et al. (Garbers et al. 2011). Consequently, the levels of sIL-6R and sgp130 must be markedly lower than that of IL-6 in order to avoid inhibition on IL-6 classic signaling. In this study, we assigned 50 ng/ml as the appropriate concentration of sIL-6R, which can induce IL-6 trans-signaling without affecting classic signaling when all sIL-6R were trapped by sgp130 in the form of IL-6/sIL-6R/sgp130.

As the natural inhibitor of IL-6-sIL-6R complexes, sgp130 exerts selective inhibition on IL-6 trans-signaling without affecting the membrane-bound IL-6R mediated classic signaling. Kinetic parameters suggest that the IL-6-sIL-6R complex has equal affinity for membrane-bound and sgp130, and therefore, a molar excess of sgp130 is required to inhibit IL-6 trans-signaling (Jones et al. 2005; Rose-John and Neurath 2004). In the present study, we used excess amount of sgp130 (sgp130: 100 ng/ml *versus* sIL-6R: 50 ng/ml) to block IL-6 trans-signaling and found that the promotive effect on low level of RANKL-induced osteoclastic differentiation of mouse BMMs by IL-6/sIL-6R was completely abrogated, indicating that the promotion on osteoclastic differentiation is mediated by IL-6 trans-signaling but not classic signaling. However, we still can't rule out the possibility that the full achievement of physiological function of IL-6 signaling requires simultaneous activation of both classic and trans-signaling.

RANKL-RANK association and the downstream signaling cascades are crucial for osteoclastic differentiation (Gohda et al. 2005). Immunoprecipitation assay revealed that the association of RANK and TRAF6 was not changed by IL-6/sIL6R/sgp130, indicating that the regulation of osteoclastic differentiation by IL-6 signaling is achieved by interfering RANK-TRAF6 interaction. The low-level RANKL-induced expressions of NFATc1 and c-fos, two of the most pivotal transcription factors for osteoclast commitment, as well as osteoclast-specific genes were also promoted by IL-6/sIL-6R and suppressed by addition of sgp130. These facts imply that the mechanisms underlying IL-6 signaling regulation of osteoclastic differentiation is

downstream of RANK-RANKL interaction and upstream of osteoclastic transcription.

MAPKs and NF-κB signaling pathways are known to be implicated in RANKL-RANK signaling transduction and are required for subsequent osteoclast formation (Ang et al. 2011; Ikeda et al. 2008; Tao et al. 2011). Signaling studies revealed that NF-κB and JNK activation induced by low level of RANKL was upregulated by IL-6/sIL-6R, which was thereafter suppressed by blocking IL-6 trans-signaling with sgp130. These results raise the possibility that NF-κB and JNK are involved in the cross-talk between RANK-RANK and IL-6 signaling cascades but ERK and p38 are not.

Some limitations of this current study should be mentioned. First, we did not compare the effects of sgp130 with other IL-6 signaling pathway inhibitor such as the anti-IL-6R antibody tocilizumab and the anti-trans-signaling monoclonal antibody 25F10, which will be a focus of subsequent research. Second, this study was conducted on BMMs in vitro experiments; an in vivo experiment with an animal model will be requisite to verify the results and determine the potential clinical relevance of sgp130 in inflammatory disorders.

In summary, our present study demonstrates that a selective blockage of IL-6 trans-signaling with recombinant sgp130 exhibits promising efficacy against IL-6/sIL-6R-induced enhancement of osteoclasts formation in the context of low level of RANKL. Since trans-signaling has been considered a major harmful signal contributing to IL-6-mediated inflammatory response, recombinant sgp130 or other artificially synthesized antibodies with stronger affinity to sIL-6R such as sgp130Fc may be of further interest for therapeutic drag design for inflammatory and metabolic osteolytic diseases such as rheumatoid arthritis and postmenopausal osteoporosis.

Declarations

Conflict of interest The authors declared no potential conflicts of interest with respect to the research, authorship, and/or publication of this article.

Ethical approval: All experimental procedures complied with the ARRIVE guidelines and were conducted in accordance with the guidelines for the Care and Use of Laboratory Animals of the National Institutes of Health. And all animal experiments and the use of the cell line were approved by the ethics committee of School and Hospital of Stomatology, Shandong University (No. 20210118).

References

Ang E et al (2011) Mangiferin attenuates osteoclastogenesis, bone resorption, and RANKL-induced activation of NF-kappaB and ERK. J Cell Biochem 112:89–97. doi:https://doi.org/10.1002/jcb.22800

Audet J, Miller CL, Rose-John S, Piret JM, Eaves CJ (2001) Distinct role of gp130 activation in promoting self-renewal divisions by mitogenically stimulated murine hematopoietic stem cells. Proc Natl Acad Sci USA 98:1757–1762. doi:https://doi.org/10.1073/pnas.98.4.1757

Axmann R, Bohm C, Kronke G, Zwerina J, Smolen J, Schett G (2009) Inhibition of interleukin-6 receptor directly blocks osteoclast formation in vitro and in vivo. Arthritis Rheum 60:2747–2756. doi:https://doi.org/10.1002/art.24781

Chomarat P, Banchereau J, Davoust J, Palucka AK (2000) IL-6 switches the differentiation of monocytes from dendritic cells to macrophages. Nat Immunol 1:510–514. doi:https://doi.org/10.1038/82763

Dixit A et al (2018) Frontline Science: Proliferation of Ly6C(+) monocytes during urinary tract infections is regulated by IL-6 trans-signaling. J Leukoc Biol 103:13–22. doi:https://doi.org/10.1189/jlb.3HI0517-198R

Duplomb L, Baud'huin M, Charrier C, Berreur M, Trichet V, Blanchard F, Heymann D (2008) Interleukin-6 inhibits receptor activator of nuclear factor kappaB ligand-induced osteoclastogenesis by diverting cells into the macrophage lineage: key role of Serine727 phosphorylation of signal transducer and activator of transcription 3. Endocrinology 149:3688–3697. doi:https://doi.org/10.1210/en.2007-1719

Feng W et al (2017) Combination of IL-6 and sIL-6R differentially regulate varying levels of RANKL-induced osteoclastogenesis through NF-kappaB, ERK and JNK signaling pathways. Sci Rep 7:41411. doi:https://doi.org/10.1038/srep41411

Garbers C et al (2011) Inhibition of classic signaling is a novel function of soluble glycoprotein 130 (sgp130), which is controlled by the ratio of interleukin 6 and soluble interleukin 6 receptor. J Biol Chem 286:42959–42970. doi:https://doi.org/10.1074/jbc.M111.295758

Garbers C, Aparicio-Siegmund S, Rose-John S (2015) The IL-6/gp130/STAT3 signaling axis: recent advances towards specific inhibition. Curr Opin Immunol 34:75–82. doi:https://doi.org/10.1016/j.coi.2015.02.008

Gohda J, Akiyama T, Koga T, Takayanagi H, Tanaka S, Inoue J (2005) RANK-mediated amplification of TRAF6 signaling leads to

NFATc1 induction during osteoclastogenesis. EMBO J 24:790–799. doi:https://doi.org/10.1038/sj.emboj.7600564

Heinrich PC, Behrmann I, Muller-Newen G, Schaper F, Graeve L (1998) Interleukin-6-type cytokine signalling through the gp130/Jak/STAT pathway. Biochem J 334(Pt 2):297–314

Ikeda F, Matsubara T, Tsurukai T, Hata K, Nishimura R, Yoneda T (2008) JNK/c-Jun signaling mediates an anti-apoptotic effect of RANKL in osteoclasts. J bone mineral research: official J Am Soc Bone Mineral Res 23:907–914. doi:https://doi.org/10.1359/jbmr.080211

Jones SA (2005) Directing transition from innate to acquired immunity: defining a role for IL-6. J Immunol 175:3463–3468. doi:https://doi.org/10.4049/jimmunol.175.6.3463

Jones SA, Richards PJ, Scheller J, Rose-John S (2005) IL-6 trans-signaling: the in vivo consequences. J Interferon Cytokine Res 25:241–253. doi:https://doi.org/10.1089/jir.2005.25.241

Jostock T et al (2001) Soluble gp130 is the natural inhibitor of soluble interleukin-6 receptor transsignaling responses. Eur J Biochem 268:160–167. doi:https://doi.org/10.1046/j.1432-1327.2001.01867.x

Kim GW et al (2015) IL-6 inhibitors for treatment of rheumatoid arthritis: past, present, and future. Arch Pharm Res 38:575–584. doi:https://doi.org/10.1007/s12272-015-0569-8

Kudo O, Sabokbar A, Pocock A, Itonaga I, Fujikawa Y, Athanasou NA (2003) Interleukin-6 and interleukin-11 support human osteoclast formation by a RANKL-independent mechanism. Bone 32:1–7

Lindberg MK et al (2001) Estrogen receptor alpha, but not estrogen receptor beta, is involved in the regulation of the OPG/RANKL (osteoprotegerin/receptor activator of NF-kappa B ligand) ratio and serum interleukin-6 in male mice. J Endocrinol 171:425–433. doi:https://doi.org/10.1677/joe.0.1710425

Liu XH, Kirschenbaum A, Yao S, Levine AC (2005) Cross-talk between the interleukin-6 and prostaglandin E(2) signaling systems results in enhancement of osteoclastogenesis through effects on the osteoprotegerin/receptor activator of nuclear factor-{kappa}B (RANK) ligand/RANK system. Endocrinology 146:1991–1998. doi:https://doi.org/10.1210/en.2004-1167

McInnes IB, Buckley CD, Isaacs JD (2016) Cytokines in rheumatoid arthritis - shaping the immunological landscape. Nat Rev Rheumatol 12:63–68. doi:https://doi.org/10.1038/nrrheum.2015.171

Nishimoto N, Kishimoto T (2006) Interleukin 6: from bench to bedside. Nat Clin Pract Rheumatol 2:619–626. doi:https://doi.org/10.1038/ncprheum0338

Ohsaki Y, Takahashi S, Scarcez T, Demulder A, Nishihara T, Williams R, Roodman GD (1992) Evidence for an autocrine/paracrine role for interleukin-6 in bone resorption by giant cells from giant cell tumors of bone. Endocrinology 131:2229–2234. doi:https://doi.org/10.1210/endo.131.5.1425421

Palmqvist P, Persson E, Conaway HH, Lerner UH (2002) IL-6, leukemia inhibitory factor, and oncostatin M stimulate bone resorption and regulate the expression of receptor activator of NF-kappa B ligand, osteoprotegerin, and receptor activator of NF-kappa B in mouse calvariae. J Immunol 169:3353–3362

Peters M et al (1997) Extramedullary expansion of hematopoietic progenitor cells in interleukin (IL)-6-sIL-6R double transgenic mice. J Exp Med 185:755–766. doi:https://doi.org/10.1084/jem.185.4.755

Peters M, Muller AM, Rose-John S (1998) Interleukin-6 and soluble interleukin-6 receptor: direct stimulation of gp130 and hematopoiesis. Blood 92:3495–3504

Rose-John S, Neurath MF (2004) IL-6 trans-signaling: the heat is on. Immunity 20:2–4

Rose-John S (2006) Designer cytokines for human haematopoietic progenitor cell expansion: impact for tissue regeneration.Handb Exp Pharmacol:229–247

Rose-John S, Scheller J, Elson G, Jones SA (2006) Interleukin-6 biology is coordinated by membrane-bound and soluble receptors: role in inflammation and cancer. J Leukoc Biol 80:227–236. doi:https://doi.org/10.1189/jlb.1105674

Rose-John S (2017) The Soluble Interleukin 6 Receptor: Advanced Therapeutic Options in Inflammation. Clin Pharmacol Ther 102:591–598. doi:https://doi.org/10.1002/cpt.782

Tao H, Okamoto M, Nishikawa M, Yoshikawa H, Myoui A (2011) P38 mitogen-activated protein kinase inhibitor, FR167653, inhibits parathyroid hormone related protein-induced osteoclastogenesis and bone resorption. PLoS ONE 6:e23199. doi:https://doi.org/10.1371/journal.pone.0023199

Wong PK, Quinn JM, Sims NA, van Nieuwenhuijze A, Campbell IK, Wicks IP (2006) Interleukin-6 modulates production of T lymphocyte-derived cytokines in antigen-induced arthritis and drives inflammation-induced osteoclastogenesis. Arthritis Rheum 54:158–168. doi:https://doi.org/10.1002/art.21537

Yoshitake F, Itoh S, Narita H, Ishihara K, Ebisu S (2008) Interleukin-6 directly inhibits osteoclast differentiation by suppressing receptor activator of NF-kappaB signaling pathways. J Biol Chem 283:11535–11540. doi:https://doi.org/10.1074/jbc.M607999200